



**Khayatzadeh, Saber and Flewitt, Peter E.J. and Smith, David and Tanner, David W.J. and Truman, C. E. (2017) Influence of thermal ageing on the creep behaviour of a P92 martensitic steel. Materials Science and Engineering: A, 708. pp. 544-555. ISSN 0921-5093 , <http://dx.doi.org/10.1016/j.msea.2017.10.025>**

This version is available at <https://strathprints.strath.ac.uk/62915/>

**Strathprints** is designed to allow users to access the research output of the University of Strathclyde. Unless otherwise explicitly stated on the manuscript, Copyright © and Moral Rights for the papers on this site are retained by the individual authors and/or other copyright owners. Please check the manuscript for details of any other licences that may have been applied. You may not engage in further distribution of the material for any profitmaking activities or any commercial gain. You may freely distribute both the url (<https://strathprints.strath.ac.uk/>) and the content of this paper for research or private study, educational, or not-for-profit purposes without prior permission or charge.

Any correspondence concerning this service should be sent to the Strathprints administrator: [strathprints@strath.ac.uk](mailto:strathprints@strath.ac.uk)

# Influence of Thermal Ageing on the Creep Behaviour of a P92 Martensitic Steel

Saber Khayatzadeh <sup>a,b\*</sup>, David W.J. Tanner <sup>c</sup>, Christopher E. Truman <sup>a</sup>, Peter E.J. Flewitt <sup>d</sup>, David J. Smith <sup>a†</sup>

<sup>a</sup> Department of Mechanical Engineering, University of Bristol, Bristol, BS8 1TR, UK

<sup>b</sup> Advanced Forming Research Centre, Strathclyde University, Renfrew, Glasgow, PA4 9LJ, UK

<sup>c</sup> ATKINS, The Hub, 500 Park Avenue, Aztec West, Bristol, BS32 4RZ, UK

<sup>d</sup> H H Wills Laboratory, School of Physics, University of Bristol, Bristol, BS8 1TL, UK

\* Corresponding author.

E-mail address: [saber.khayatzadeh@strath.ac.uk](mailto:saber.khayatzadeh@strath.ac.uk)

## Abstract

It is well established that thermal ageing reduces the life of engineering components operating at elevated temperature. However, there is still not an accurate approach to estimate the change in the service life as a result of thermal ageing of the material. In this study, the effect of accelerated thermal ageing, for a thousand hours prior to creep testing at a temperature of 650°C for a martensitic P92 steel has been compared to un-aged steels. The effect of thermal ageing on a primary-secondary stress dependent creep model has been explored, by conducting a set of uniaxial creep experiments on both un-aged and aged P92 steel. It was observed that thermal ageing enhanced the creep deformation for a narrow range of stresses, and systematically reduced the creep rupture life. These applied for conditions by up to a quarter of the original life. Results from creep crack growth tests for similarly aged material reduced incubation time and accelerated the crack growth rate. However, creep stress relaxation tests revealed no evidence of the influence of thermal ageing on rate of relaxation.

**Keyword:** Thermal Ageing, P92 steel, Creep Deformation, Creep Stress Relaxation, Creep Crack Incubation

## 1. Introduction

Depending on the specific application a variety of different steels have been used for conventional, and nuclear electrical power generating plant components operating at high temperature for long periods of service. Therefore the evaluation of the structural integrity assessment of such components is important, especially after being exposed to high temperature for long times [1]. It is well established that small extended periods of operation at temperatures and service loads potentially degrades the microstructure and associated mechanical and physical properties. These changes can significantly modify the remaining creep life of the components [2]–[8]. As a consequence, one of the major challenges for extending the life of components operating at elevated temperature is to understand the changes in the microstructure and the associated mechanical response of these structural materials caused by thermo-mechanical history [2], [3], [9]. Investigating how the creep deformation and fracture behaviour of the material and components are influenced by these changes is a significant topic of theoretical and practical interest [9].

---

† In memory of Professor David Smith, who died as the result of a tragic climbing accident during the period this work was undertaken.

## Symbols:

$E$	Young's Elastic Modulus (GPa)
$Z$	Elastic Follow-Up Factor
$a$	Material Property
$A_p$	Material Constant for Power Law Primary Creep
$A_s$	Material Constant for Power Law Secondary Creep
$B$	Material Property
$B_n$	Compact Tension Net Specimen Thickness (mm)
$C_{MG}$	Monkman-Grant Constant
$\varepsilon_c^{Total}$	Total Creep Strain
$\varepsilon_f$	Failure Strain
$\dot{\varepsilon}_c$	Creep Strain Rate
$\dot{\varepsilon}_{avg}$	Average Creep Strain Rate
$\dot{\varepsilon}_{min}$	Minimum Creep Strain Rate
$m$	Material Property
$m_p$	Time Exponent for Power Law Primary Creep
$m_s$	Time Exponent for Power Law Secondary Creep
$n_p$	Stress Exponent for Power Law Primary Creep
$n_s$	Stress Exponent for Power Law Secondary Creep
$P$	Applied Load (KN)
$P_L$	Rigid-Plastic Limit Load (KN)
$t$	Time (s)
$t_r$	Rupture Time (s)
$t_i$	Incubation Time (s)
$W$	Compact Tension Specimen Width (mm)
$\sigma$	Stress (MPa)
$\sigma_y$	Yield Stress (MPa)
$\sigma_{ref}$	Reference Stress (MPa)

The growing demand to increase the efficiency of electrical power generating plants and reduce the CO<sub>2</sub> gas emissions, has led to an increase in the operating temperature and pressure in the boilers [1-4]. This intent sets the need to adopt steels with improved creep resistance such as versions of the 9%Cr0.5%Mo martensitic and ferritic steels, e.g. P91 and P92. Certainly additions of elements such as tungsten and boron increase the creep strength [12]. In this context P92 steel is one of the commonly considered high Cr, creep resistant steels [1–4]. Since these types of steel have been developed particularly to operate at elevated temperature, it is important to be able to provide procedures to evaluate service life with high confidence [1].

To determine the influence of long term thermal ageing on the behaviour of steel, several studies have been conducted on P92 steel to explore the evolution of microstructure by holding steel specimens for a variety of times from short to relatively long periods in the absence of stress at temperatures in the range of 600°C and 650°C [2], [3], [5]–[8]. In a comprehensive review conducted by Hald [3], it was reported that the main precipitates in P92 steel that form often prolong ageing are M<sub>23</sub>C<sub>6</sub>, MX and Laves phase, where the M<sub>23</sub>C<sub>6</sub> carbide precipitates form mainly during tempering. The M<sub>23</sub>C<sub>6</sub> carbide precipitate is a combination of carbon with the elements including Cr, Fe, Mo or W. The precipitation of MX is generally in the form of (V, Nb)(N, C) carbo-nitride [3]. The Laves phase, with the form of (Fe, Cr)<sub>2</sub>(Mo, W), is thermodynamically unstable at typical tempering temperatures, and forms at plant operating temperatures [3]. It is proposed that the probability of Laves phase precipitating decreases as the tempering temperature approaches 800°C [16]. Gustafson et al [5] explored the influence of coarsening of both M<sub>23</sub>C<sub>6</sub> and MX precipitates, in a P92 steel aged at 600°C and

650°C for period between 1000 to 26000 hours. In general even short ageing periods of about 1000 hours were found to be sufficient to generate changes in the microstructure. Several studies have evaluated precipitate evolution in 9 to 12% Cr steels [2]–[9], [13], and the mechanisms that influence thermal ageing on microstructure. Nevertheless, few studies have examined specifically the effect of thermal ageing on the creep deformation [4], [2], [3], [5]–[8]. Hence there remains a need to understand of how these changes affect the mechanical response of specific steels such as P92 within the creep regime, especially in the presence of a crack, and during in-service stress relaxation [1]. Paniat et al [4] examined the creep deformation of aged T92 steel that had been soaked at a defined test temperature, over a limited range of high stresses. Other works [2]–[8] have proposed that thermal ageing, under laboratory conditions, is sufficient to induce changes in the microstructure and creep deformation.

In practice service components operating at high temperature are subject to a wide range of stress states, especially in the presence of geometrically non-linearities, such as a crack [1], [17] [18]. Certainly, the creep deformation and fracture mechanisms for 9% Cr 1% Mo steels when subjected to low levels of stress, responded differently compared to when exposed to high stresses [16], [17] [18]. It is common to consider conventional creep models presuming one mechanism operates across all the stress levels [10], [12], [15], [19]–[22]. However these approaches neglect the effect of thermal ageing. To evaluate the effect of thermal ageing on creep behaviour it is important to consider the stages of both primary creep and secondary creep, especially since the P92 steels exhibit significant primary creep strain [1], [18]. To overcome this difficulty, a primary-secondary stress dependent creep model has been developed by Khayatadeh et al [1], [18] which takes into account creep behaviour for an un-aged steels over for a wide range of applied stresses from 40MPa to 170MPa at 650°C [18]. This model is now employed to investigate the effect of thermal ageing on creep deformation over a wide range of stresses.

In the present paper, the effect of thermal ageing on creep deformation, creep crack incubation and growth, for creep stress relaxation of martensitic P92 steel is investigated. The experimental results are discussed and compared with model predictions.

## 2. Material and Experimental Procedures

### 2.1. Material

The material for this research was ASME steel grade P92 extracted from base material at the end section remote from a circumferential weld in a pipe with an inner and outer diameter of 290mm and 350mm [1]. Table 1 shows the chemical composition of P92 steel [23]. The pipe was normalised at a temperature of 1070°C for a period of 45 minutes and then tempered at 780°C for 105 minutes. A post-weld heat treatment was conducted at a temperature of 760°C for 180 minutes [1]. At this stage the aged specimens were soaked in a furnace for 1000 hours at 650°C at the same temperature as the test condition selected for performing creep tests. For consistency, to provide a similar condition for aged steel, all the specimens were heat treated together after manufacturing process to ensure all were equally thermally aged.

Table 1: Chemical composition of P92 (wt %) [23]

Ni	C	Mn	P	S	Si	Cr	W	Mo	V	Nb	N	B	Al	Fe
0.27	0.10	0.45	0.015	0.002	0.45	8.62	1.86	0.33	0.21	0.076	0.047	0.003	0.019	Bal.

## 2.2. Mechanical Tests

### 2.2.1. Forward Creep

Standard round bar uniaxial creep specimens were extracted parallel to the axis of the pipe remote from the weld to ensure a uniform microstructure [1]. Since in-service the P92 steel pipe is subjected to an internal pressure of about 30MPa at temperature of 625 to 630°C [24], the creep tests were conducted within a range of stresses from low (40MPa) to relatively high (170MPa) at 650°C for both the un-aged and aged conditions. Two tests were taken to rupture at stresses of 120MPa and 170MPa for both aged and un-aged conditions. The remainder of tests were interrupted after reaching and progressing in the secondary creep regime, thereby allowing the minimum creep strain rate to be determined. All the tests were conducted under elastic creep conditions. The yield stress was measured to be approximately 273MPa at 650°C for both un-aged and aged conditions (as discussed in 3.1 [1]). Table 2 summarizes the details of the creep tests conducted at constant load.

Table 2: Details of uniaxial creep tests on aged and un-aged P92 steel at 650°C [1]

Test ID	Material Condition	Nominal Stress (MPa)	Failure Strain (%)	Rupture Time (hr)
P92-T1	Un-Aged	170	34.5	7.2
P92-T2		120	16.6	807
P92-T3		100	----	----
P92-T4		80	----	----
P92-T5		60	----	----
P92-T6		40	----	----
P92-TA1	Aged	170	35.4	7.4
P92-TA2		120	28	330
P92-TA3		100	----	----
P92-TA4		80	----	----
P92-TA5		60	----	----

### 2.2.2. Creep Crack Growth

Creep crack growth tests at constant load were conducted at three different levels of load for un-aged and aged P92 steel specimens (as tabulated in Table 3). The specimens were extracted from the end of the pipe (parent side) with the notch oriented tangential to the curvature [1], [25]. All the compact tension (C(T)) specimens were manufactured based on ASTM 1457 [26] and used a screw loading test rig (Fig. 1) [1]. A screw loaded design was selected, so that they could also be used for elastic follow-up tests. The reason for choosing this design is because pin loaded C(T) specimens when used in a three bar structure relax residual stresses, while screw loaded specimens does not. The details of creep crack growth tests under elastic follow-up, and full rig details are given in [1]. It should be noted that Shirahatti [27] concluded that a screw loaded specimen produces more bending of the loading bars compared to pin loading. There was a negligible differences for displacements up to 0.4mm. Therefore, with small displacements during either crack initiation or propagation, the effect of bending is small. Since the aim of this study is to predict creep crack initiation, the influence of bending can be neglected. Simulations conducted by Khayatzaheh [1] on pin and screw loading showed similar results.

All the C(T) specimens contained twenty percent depth side grooves and a 2mm of pre-crack introduced by electro-discharge machining (EDM) with 0.1mm dia wire. Some of the C(T) specimens were aged at 650°C for 1000 hours after manufacture, as discussed earlier. Load line displacement (LLD) was recorded using a linear variable differential transducer (LVDT) and the amount of creep crack growth evaluated using an electrical direct current potential drop (DCPD) system (full details of the calibration procedure can be found in [1], [27]).

Table 3: Details of the creep crack growth tests for aged and un-aged P92 steel

Test ID	Material Condition	W (mm)	B (mm)	B <sub>n</sub> (mm)	a/w	Load (KN)	Plane Stress-Reference stress (MPa)	K (MPa√m)
LC-1-UnAged	Un-Aged	38	19	15.4	0.5	6.25	120	16.66
LC-1-Aged	Aged	38	19	15.4	0.5	6.25	120	16.66
LC-2-UnAged	Un-Aged	38	19	15.4	0.5	4.17	80	11.11
LC-2-Aged	Aged	38	19	15.4	0.5	4.17	80	11.11
LC-3-UnAged	Un-Aged	38	19	15.4	0.5	3.12	60	8.32
LC-3-Aged	Aged	38	19	15.4	0.5	3.12	60	8.32

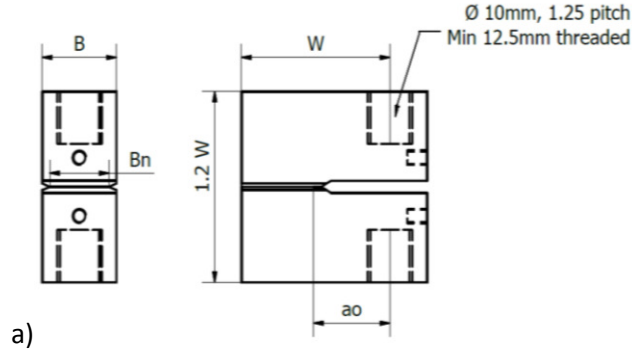


Fig. 1: a) Schematic of screw load C(T) specimen; all symbols are described in the text.

The reference stress,  $\sigma_{ref}$ , definition based on the limit load was employed to estimate the stress in a cracked component.

$$\sigma_{ref} = \sigma_y \frac{P}{P_L} \quad (1)$$

where  $\sigma_y$ ,  $P$ , and  $P_L$ , are yield stress, applied load, and rigid-plastic limit load. For a C(T) specimen, the reference stress can be defined by [1], [28]:

$$\sigma_{ref} = \frac{P}{W B_n \eta_L} \quad (2)$$

where  $W$ ,  $B_n$ , and  $a$  are the specimen width, net specimen thickness, and the crack length.

$\eta_L$  for plane stress is given by:

$$\eta_L = \sqrt{(1 + \gamma) \left(1 + \gamma \left(\frac{a}{W}\right)^2\right)} - \left(1 + \gamma \left(\frac{a}{W}\right)\right) \quad (3)$$

where  $\gamma = \frac{2}{\sqrt{3}}$  ( $0 \leq a/W \leq 1$ )

and for plane strain:

$$\eta_L = \gamma \left[ \sqrt{2.702 + 4.599 \left(\frac{a}{W}\right)^2} - \left(1 + 1.702 \left(\frac{a}{W}\right)\right) \right] \quad (4)$$

where  $\gamma = \frac{2}{\sqrt{3}}$  ( $0.09 \leq a/W \leq 1$ )

It is noteworthy that in the present research plane stress-reference stress criterion was applied since the manufactured compact tension specimen was sufficiently thin to not satisfy a plane-strain criterion.

### 2.2.3. Uniaxial Creep Stress Relaxation

Uniaxial creep stress relaxation tests with an elastic follow-up factor of  $Z=1.17$  were conducted on un-aged and aged P92 steels at 650°C to examine the effect of thermal ageing [18]. The initial residual stress, in this

test rig, was introduced by applying a misfit to a level of 123MPa. Uniaxial test specimens were extracted and manufactured from the pipe following a similar approach applied for the uniaxial creep specimens (see Section 2.2). Table 4 provides the details of the uniaxial creep stress relaxation tests conducted on both the un-aged and aged specimens at 650°C. Full details about the procedure for performing the tests can be found in [1][18], [29], [30].

The purpose of this research is to study creep stress relaxation at a very low elastic follow-up condition. Therefore, a test rig was designed in such a way that it provided the lowest feasible elastic follow-up factor that could be achieved within the constraints of manufacture. This accounts for the value of 1.17 as the elastic follow-up factor.

Table 4: Details of creep stress relaxation tests for un-aged and aged P92 steels at 650°C

Test ID	EFU Factor (Theoretical)	Material Condition	Type of Residual Stress	$\sigma_{initial}$ (MPa)	Duration of Test (hr)	$\sigma_{final}$ (MPa)
EFU-1	1.17	Un-Aged	Misfit	123	584	39
EFU-2	1.17	Aged	Misfit	123	768	38

### 3. Results

In the un-aged condition the P92 steel had a martensitic microstructure with a prior austenite grain size of  $\sim 35\mu m$  (mean linear intercept). This mean grain size was not changed by thermal ageing and there was evidence of second phase precipitation [1].

#### 3.1. Influence of Thermal Ageing on Mechanical Properties

Tensile tests were conducted at a temperature of 650°C for both un-aged and aged P92 steel specimens to evaluate the mechanical properties [1], as summarised in Table 5. Fig. 2 shows the true stress-strain curve for un-aged and aged P92 steel specimens at 650°C. There was no change in the Young modulus of elasticity and the yield point within experimental error, but the ultimate stress reduced by about 4%. This is in consistent with other researchers findings that thermal ageing for the conditions selected did not modify mechanical properties significantly [4], [31]. Also, as demonstrated, the work hardening rate, up to 0.05 strain, decreases in the aged condition and is lower than the un-aged.

Table 5: Details of tensile tests on un-aged and aged P92 steel at 650°C

Material Condition	Temperature	Strain Rate (1/sec)	$E$ (GPa)	$\sigma_{0.2\%}$ (MPa)	$\sigma_{uts}$ (MPa)
Un-Aged	650°C	7.82e-4	120	273	293
Aged		9.25e-4			279

#### 3.2. Creep Deformation and Stress Relaxation

Creep deformation for un-aged and aged P92 specimens at 650°C was studied by conducting a set of forward creep tests at constant load over a wide range of applied stresses. As Fig. 3 shows, there was no difference in the secondary creep rate for un-aged and aged conditions at stresses of 170MPa (Fig. 3a), 80MPa and 60MPa (Fig. 3d). However, a difference in rate was observed at stresses of 120MPa (Fig. 3b) and 100MPa (Fig. 3c). As shown in Fig. 3b, there was a substantial difference in the primary and secondary creep behaviour for both un-aged and aged (1000 hours of thermal aging) P92 steel at 120MPa. This reduced the creep life by almost a third compared with un-aged material together with a reduction in rupture time and an increase in minimum secondary creep strain rate. It is apparent that reducing in the applied stress from 120MPa to 100MPa, the effect of thermal ageing was reduced. Analysis of the creep curves for stresses at 80MPa and 60MPa, reveals

that thermal aging did not affect the primary-secondary creep behaviour at low stress for the period of testing conducted. Moreover, the experimental creep curves at 100MPa and 120MPa, indicate that thermal aging does not influence the primary creep, but accelerates the rate of secondary creep.

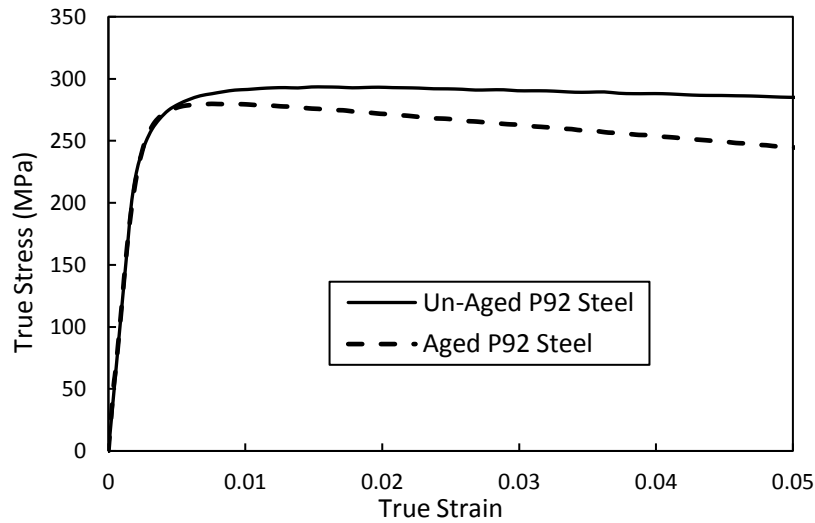


Fig. 2: True stress-strain curves for un-aged and aged P92 steel at 650°C

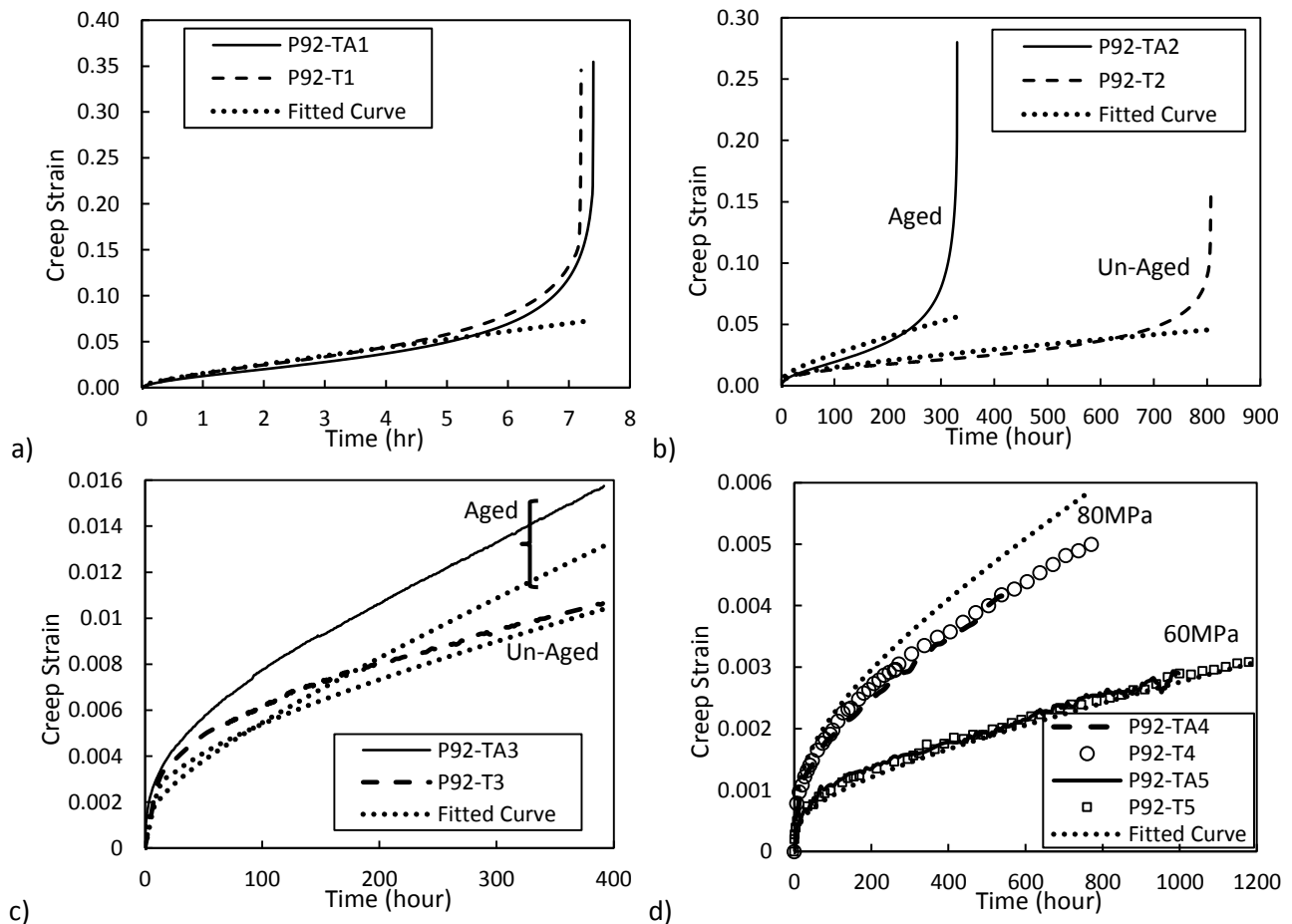


Fig. 3: Creep curves for un-aged and aged P92 steel at 650 °C, a) 170MPa, b) 120MPa, c) 100MPa, d) 80MPa and 60MPa



The minimum and average creep strain rates for both the un-aged and aged P92 steel specimens are given in Table 6. All the forward creep tests were terminated at a point that would provide confidence in a value for the minimum creep strain rate; except 120MPa and 170MPa tests which were taken to rupture. The minimum creep strain rate,  $\dot{\epsilon}_{min}$ , and average creep strain rate,  $\dot{\epsilon}_{ave}$ , can be obtained from [1], [32]:

$$\dot{\epsilon}_{min} = A_s \sigma^{n_s} \quad (5)$$

$$\dot{\epsilon}_{ave} = \epsilon_f / t_r \quad (6)$$

where  $\sigma$ ,  $A_s$ ,  $n_s$  are applied stress, material constants for power law creep during the secondary stage, and  $\epsilon_f$  and  $t_r$  are the failure strain and rupture time, respectively. Average creep strain rates for both stress levels of 120MP and 170MPa up to failure were computed. The average creep strain rate for un-aged and aged steel was very close at a stress level of 170MPa, while at 120MPa, this value was four times higher for aged test specimens compared to un-aged [18]. Fig. 4 shows the minimum creep strain rate plotted against applied stress for un-aged and aged P92 steel at 650°C. This increase in creep strain rate was reduced for a stress level of 100MPa whereas for stresses at 80MPa and below, no difference was observed. The un-aged and aged steels generally showed a behaviour consistent with the results of other workers [4], [15], [24], [33]–[35], whereas for some stresses the aged specimens exhibit a higher creep rate compared to un-aged steel.

Fig. 5 shows the experimental results for uniaxial creep stress relaxation for un-aged and aged P92 steels with initial residual stress. For both tests, the initial residual stress of 123MPa relaxed to a similar value, however specimen EFU-2 (aged P92) had to be tested for almost 200 hours more to achieve a similar level of relaxation, see also Table 4.

Table 6: Minimum and average creep strain rates for un-aged and aged P92 steels at 650°C

Material Condition	Stress (MPa)	40	60	80	100	120	170
	Test ID	<b>P92-T6</b>	<b>P92-T5</b>	<b>P92-T4</b>	<b>P92-T3</b>	<b>P92-T2</b>	<b>P92-T1</b>
Un-Aged	$\dot{\epsilon}_{min}$ (1/hr)	3.41e-7	1.20e-6	3.48e-6	1.27e-5	3.73e-5	8.00e-3
	$\dot{\epsilon}_{ave}$ (1/hr)	----	----	----	----	2.06e-4	4.8e-2
	Test ID	----	<b>P92-TA5</b>	<b>P92-TA4</b>	<b>P92-TA3</b>	<b>P92-TA2</b>	<b>P92-TA1</b>
Aged	$\dot{\epsilon}_{min}$ (1/hr)	----	1.20e-6	3.48e-6	2.64e-5	1.25e-4	7.30e-3
	$\dot{\epsilon}_{ave}$ (1/hr)	----	----	----	----	8.48e-4	4.79e-2

### 3.3.Creep Crack Incubation:

Since there is an influence on creep deformation behaviour arising from thermal ageing over a specific range of stresses (see Section 3.2), it is also important to understand the effect of thermal ageing on creep crack incubation and growth. Table 7 summarises the experimental results gained from the creep crack growth tests conducted at constant load conditions using un-aged and aged P92 steels test specimens at 650°C. Notably, the final crack length for the aged specimen was greater compared to the corresponding tests on the un-aged specimen. The incubation times for both 0.1mm and 0.2mm defined lengths and the final crack length for each test are shown in Table 7. In the present research, 0.1mm of crack extension was selected to define the initiation limit as this corresponds to a mean value change in the slope of the curve for crack extension, in terms of voltage ratio, against total load line displacement, as described in Fig. 6a \*. This curve, for test

\* It should be noted that 0.2mm is an accepted criteria in the literature and is used in this paper where comparing results with published data.

specimen LC-1-UnAged, represents both loading and creep regions. The corresponding creep crack incubation point is identified in Fig. 6a. Also, this length was detectable using the DC-PD system. During the loading, no effect of plastic deformation was observed [1].

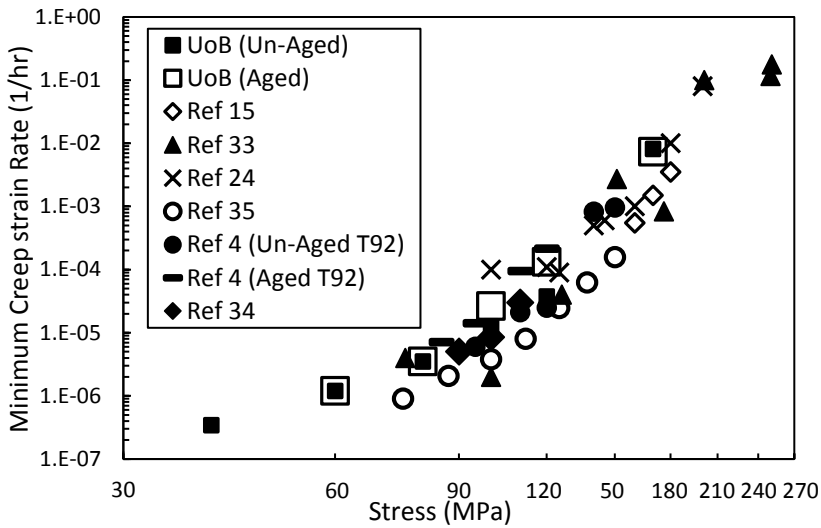


Fig. 4: Minimum creep strain rate against the applied stress level for un-aged and aged P92 steels at 650°C, compared with earlier studies (UoB indicates the results obtained by the present research)

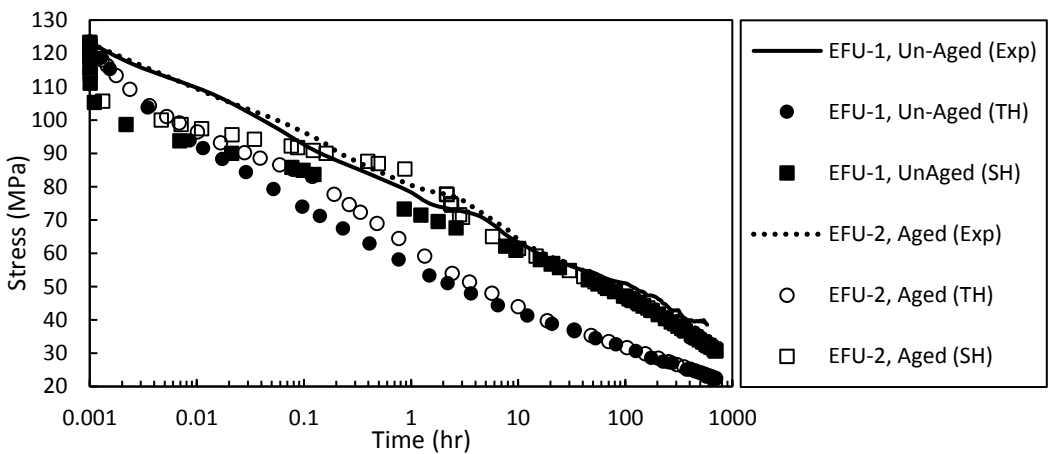


Fig. 5: Stress relaxation curve and predictions for un-aged and aged specimens with 123MPa initial residual stress and EFU=1.17

Table 7: Experimental results of creep crack growth tests for un-aged and aged P92 steel at 650°C

Test Number	Plane Stress-Reference Stress (MPa)	Total Creep Time (hr)	Time to Initiate 0.1mm Crack Growth, $t_i$ (hrs)	Time to Initiate 0.2mm Crack Growth, $t_i$ (hrs)	Final Crack Length (mm)
LC-1-UnAged	120	125	49	74	0.76
LC-1-Aged	120	125	39	63	1.19
LC-2-UnAged	80	1500	249	340	2.37
LC-2-Aged	80	1500	160	295	2.78
LC-3-UnAged	60	2772	800	1100	0.95
LC-3-Aged	60	2772	400	752	1.04

Fig. 6b, c and d show the extension of the creep cracks in the C(T) specimens for un-aged and aged steel specimens for a plane stress-reference stresses of 120MPa, 80MPa, and 60MPa at 650°C. As revealed in Table

7, the final creep crack length, after terminating a creep test, for aged steel is higher compared to the un-aged. As expected the crack growth rate is faster at higher reference stress, regardless of the state of steel. Hence creep crack incubation time is reduced by the effect of ageing and then the crack propagates faster; this was more evident for high levels of applied load (e.g. plane stress-reference stress of 120MPa, and 80MPa).

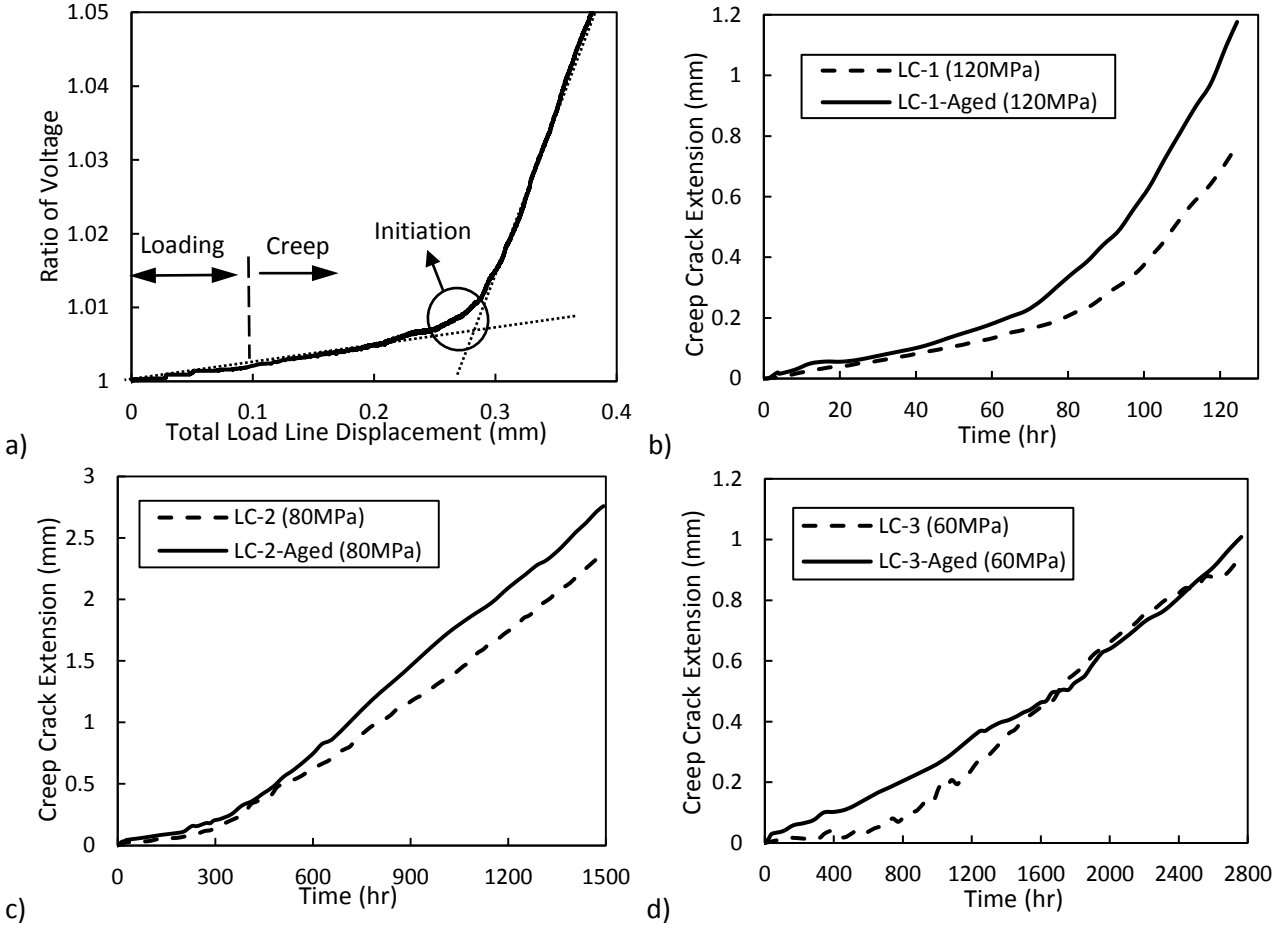


Fig. 6: a) Ratio of voltage against total load line displacement, including loading and creep, for test LC-1-UnAged showing the definition of crack initiation. b, c and d) Creep crack extension with time for un-aged and aged C(T) specimens at plane stress-reference stress of 120MPa, 80MPa, and 60MPa, respectively.

Fig. 7a shows the creep crack growth rate against the creep time for un-aged and aged P92 steels where the rate of growth decreased as the reference stress (or load) was reduced. A substantial difference in the crack growth rate between the two conditions was not observed at the plane stress-reference stress of 120MPa. While this was higher for aged steel compared to un-aged material at 80MPa and this difference was increased for 60MPa. Differences were noted in the creep properties for stresses  $40\text{MPa} < \sigma < 85\text{MPa}$ , whereas there was no difference between un-aged and aged creep properties. However, it is noteworthy that in the range of  $85\text{MPa} < \sigma < 140\text{MPa}$  the deformation rate was higher for the aged steel.

Fig. 7b illustrates the creep crack growth rate as a function of the creep crack extension for un-aged and aged P92 steel specimens; where the minimum creep crack growth rate was achieved at a similar value for 0.1mm of crack growth, except for LC-1-UnAged specimen where it occurred around 0.2mm. These values were lower for un-aged steel compared to aged and reduced as the level of load decreased (Fig. 7a). As shown, once the crack had initiated, the minimum value for creep crack growth rate increased as the crack propagated.

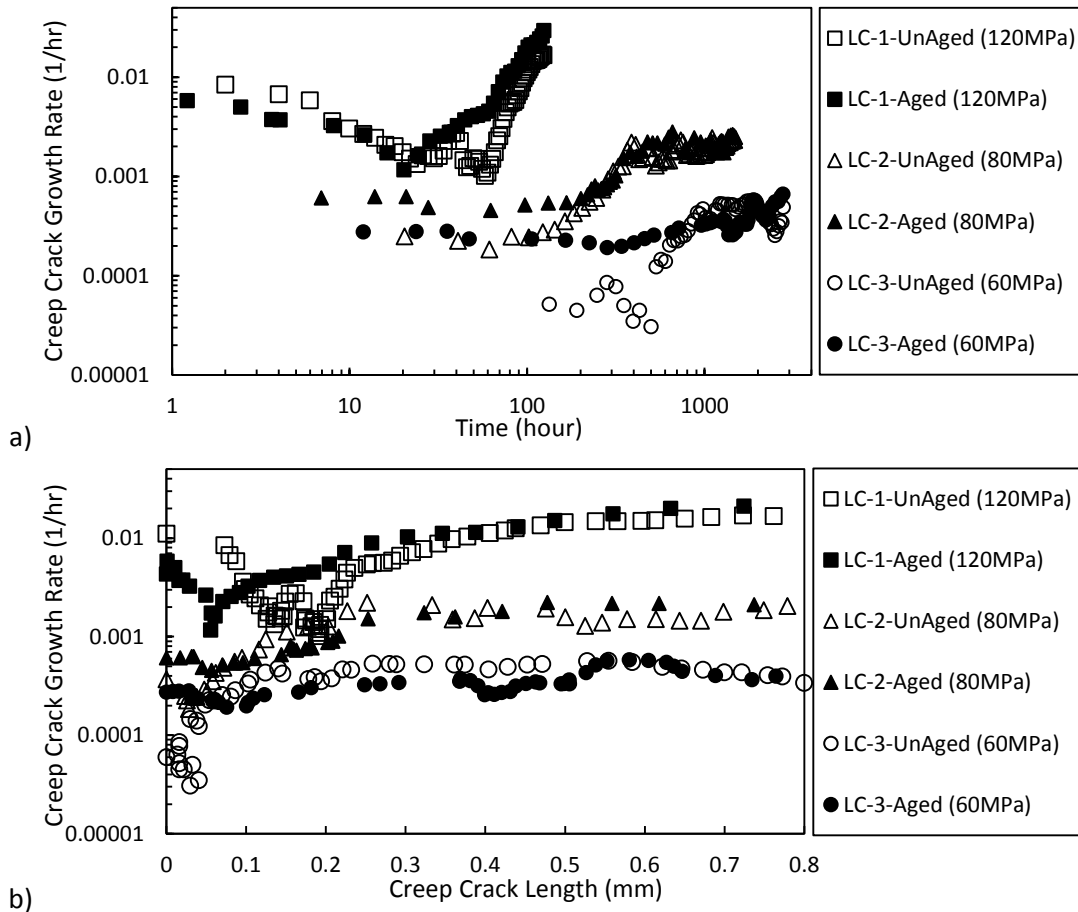


Fig. 7: Comparing creep crack growth for un-aged and aged P92 steels at 650°C. a) Creep crack growth rate against creep time, b) Creep crack growth rate against creep crack length. (The plane stress-reference stress indicated for each test in the brackets)

Once the creep crack growth tests were completed, all the C(T) specimens were sectioned longitudinally into three slices, using EDM machining with 0.1mm dia wire. One thin slice (2mm thick) was extracted from the middle of the C(T) specimen and two other removed slices equal in thickness either sides were opened to measure crack length [1]. The surface of the middle slice was ground, polished and etched for microstructural analysis over the area surrounding the crack tip. The specimens were etched using Vilella's reagent (1gr picric acid, 5ml hydrochloric acid and 100ml ethanol). Fig. 8a and Fig. 8b compare the fracture surfaces for un-aged and aged specimens subjected to identical plane stress-reference stresses of 120MPa. Specimen LC-1-UnAged (Fig. 8a) has a well-defined crack front related to the extent of crack growth, while specimen LC-1-Aged, thermally aged for 1000 hours, contains irregular crack front. These correspond with the final crack length for the aged specimen compared to the un-aged specimen (Table 7). A similar behaviour between un-aged and aged specimens was observed for other reference stresses of 80MPa and 60MPa. Fig. 8c shows an optical micrograph of the crack path in the etched slice, removed from the middle of the aged P92 C(T) specimen at plane stress-reference stress of 80MPa. There were more microcracks and branches in the aged steel. The distribution of intergranular cracks is consistent with creep cavities forming on those prior austenite boundaries oriented perpendicular to the applied stress.

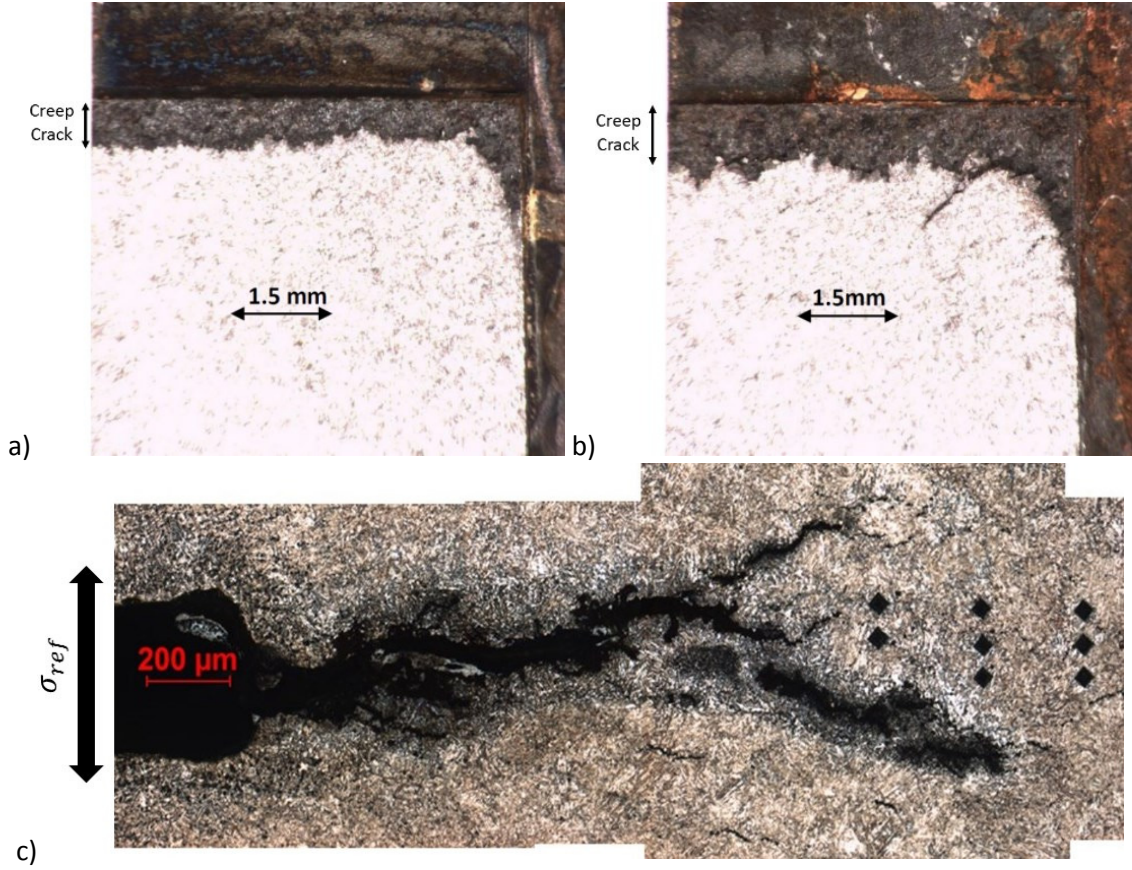


Fig. 8: a and b) Comparison of crack front C(T) specimens at 120MPa plane stress-reference stress for un-aged and aged conditions, respectively. c) Optical image of the crack path on the etched sides, removed from the middle of the C(T) specimen at plane stress-reference stress of 80MPa for aged condition (LC-2-Aged).

## 4. Discussion

### 4.1. Creep Deformation Over a Range of Stresses

The forward creep tests for aged and un-aged conditions reveal that, thermal ageing has effect on creep deformation over only a limited range of stresses (see Section 3.2). This effect was restricted to secondary and tertiary creep range. To evaluate creep deformation for the aged steels, it is necessary to have a comprehensive creep model that accommodates all these contributions. Hence, a primary and secondary stress dependent creep model, similar to the model developed by Khayatzaheh et al [18], was employed to explore the effect of thermal ageing on stress dependent creep regimes. The model considers three stress dependent creep regimes; region *I*, stresses between 40MPa to 85MPa, region *II*, stresses between 85MPa to 140MPa, and region *III*, stress levels above 140MPa. Fig. 9 shows the minimum (secondary) creep strain rate change with applied stress for un-aged and aged P92 steel with expected stress ranges for each creep regime and estimated slope. It is evident that there are two changes in the slope representing changes in creep properties. Due to lack of experimental data, properties to region *I* were extrapolated for stresses below 40MPa.

The general form of total creep strain ( $\epsilon_C^{Total}$ ), based on the power law theory that includes only primary and secondary creep, is employed, hence [18]:

$$\epsilon_C^{Total} = \epsilon_{primary} + \epsilon_{secondary} = A_p \sigma^{n_p} t^{m_p} + A_s \sigma^{n_s} t^{m_s} \quad (7)$$

where  $A_p$ ,  $n_p$ , and  $m_p$  ( $0 < m_p < 1$ ) are material constants for power law creep during the primary stage, and  $A_s$ ,  $n_s$ , and  $m_s$  ( $m_s = 1$ ) are material constants for power law creep during the secondary stage. The creep properties for primary and secondary creep of each creep regime (for un-aged and aged P92 steel) were computed, using Eq. 7, and tabulated in Table 8. Since that thermal ageing did not affect the creep deformation for stresses within regions *I* and *III*, similar creep properties for un-aged and aged P92 steel were considered. The experimental data are spread for the two conditions and the stress levels for the transitions from one regime to another regime are not well defined.

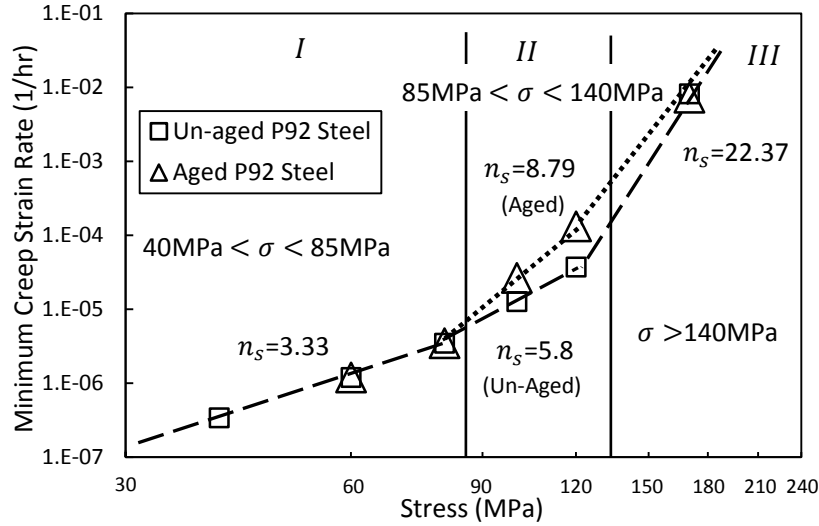


Fig. 9: Minimum creep strain rate against the applied stress level for only un-aged and aged P92 steel at 650°C (UoB indicates the results obtained by the present research)

Table 8: Creep properties for aged and un-aged P92 steel at a wide range of stresses at 650°C

Creep Regimes	Un-Aged P92 Steel					Aged P92 Steel				
	Secondary Creep		Primary Creep			Secondary Creep		Primary Creep		
	$A_s$	$n_s$	$A_p$	$n_p$	$m_p$	$A_s$	$n_s$	$A_p$	$n_p$	$m_p$
$40 < \sigma < 85 \text{MPa}$	1.50E-12	3.33	8.20E-10	3.05	0.28	1.50E-12	3.33	8.20E-10	3.05	0.28
$85 < \sigma < 140 \text{MPa}$	2.73E-17	5.8	8.20E-15	5.60	0.26	5.49E-23	8.79	1.25E-20	8.43	0.285
$140 \text{MPa} < \sigma$	1.00E-52	22.37	1.49E-49	20.94	0.35	1.00E-52	22.37	1.49E-49	20.94	0.35

The creep strain curves at a variety of stress levels, using Eq. 7, for a combination of primary and secondary creep regions were computed and compared with experimental results, as shown in Fig. 3 where the fitted curve represents the predictions for creep deformation. Since the creep properties were considered to be identical at creep regime *I* and *III* for both aged and un-aged P92 steel, only one fitted curve is presented for predictions of creep deformation (Fig. 3a, Fig. 3b and Fig. 3d). The comparison between experimental and fitted curves shows a good agreement.

Among the predicted curves over a wide range of stresses (Fig. 3), only at stress level of 100MPa a poor agreement was observed between experiment and prediction (Fig. 3c). One of the factors that would influence this difference could be the uncertainties associated with defining the turning points (Fig. 9) [18] for aged material. An identical turning point for un-aged material, defined in [18], has been applied for aged material. However, there is no evidence of influence of thermal ageing on turning points, due to lack of experimental

data. Therefore, defining the creep properties for aged material within the regime based on un-aged material, may account for inaccuracy in predictions at 100MPa.

To predict the influence of thermal ageing on creep stress relaxation, a similar model for creep stress relaxation to [18] was employed using the stress dependent creep properties for un-aged and aged steels. This model takes into account both strain hardening and time hardening approaches. Creep stress relaxation ( $d\sigma$ ) is the conversion of elastic strains to creep strain in the presence of elastic follow-up:

$$d\sigma = -\frac{E}{Z} \dot{\epsilon}_c dt \quad (8)$$

where  $\dot{\epsilon}_c$  and  $Z$  are the rate of creep strain and elastic follow-up factor, respectively. Normally, primary and secondary creep strain are considered during the relaxation since it is unlikely the tertiary creep is reached [29] [18]. For time hardening, the creep strain rate is described as a function of stress, temperature, and time, and based on Eq. 5, it can be expressed as:

$$\dot{\epsilon}_c = A_p \sigma^{n_p} m_p t^{m_p-1} + A_s \sigma^{n_s} \quad (9)$$

Considering the strain hardening approach, defining the creep strain rate as a function of stress, temperature, and creep strain accumulation, gives [18]:

$$\dot{\epsilon}_c = A_p^{1/m_p} \sigma^{n_p/m_p} (m_p \epsilon_c)^{(m_p-1)/m_p} + A_s \sigma^{n_s} \quad (10)$$

Predictions of creep stress relaxation with  $Z=1.17$  for un-aged and aged conditions were performed by considering the primary-secondary stress dependent creep model within a finite element simulation [18]. The predictions shown in Fig. 5 for un-aged and aged P92 martensite steel using either time hardening or strain hardening are close to each other, except at round 85MPa where the model predicted less stress relaxation for aged condition over the time. Furthermore both steels approached a same trend after a short period of time. In general for the material conditions considered here, strain hardening provided more accurate predictions compared to time hardening.

Overall, there was little difference between the uniaxial creep stress relaxation curves of un-aged and aged steels for both the experimental measurements and FE model predictions. This was due to rapid stress relaxation in the early stages of creep deformation. The main difference between creep properties of un-aged and aged steels was in a stress range between 85MPa to 140MPa. Therefore, as soon as the stress level decreased to below 85MPa, both steels followed the similar properties.

## 4.2. Critical Creep Load Line Displacement

Load line displacement has been used previously by Ainsworth [36] as a parameter to represent strain accumulation localised to the crack tip within a component. This method has been employed for un-aged and aged P92 steels at elevated temperatures [1]. However, creep load line displacement is a parameter which is a function of creep strain accumulation around the crack tip. Once it reaches a critical value, this is equivalent to the creep damage being sufficient to create a small but known crack extension [1]. The progress of creep load line displacement for un-aged and aged C(T) specimens for a range of loads is considered in Fig. 10a with the corresponding incubation time for each test highlighted. The experimental results reveal that un-aged specimens exhibit a higher creep load line displacement compared to the aged condition. Also, less creep strain accumulation was introduced to incubate crack growth when the specimen was aged compared to un-aged specimens. This level of accumulation decreased as the load was decreased. Also, a higher reduction was

observed for aged compared to the un-aged condition. Since the geometry of specimens and loading condition for both conditions of steel was identical, the stress field around the crack tip prior to the incubation are similar. However, each stress field around the crack tip would experience different creep strain accumulation depending on which creep regime was operating. The difference between the un-aged and aged conditions was mainly observed for the stress range of 85MPa to 140MPa, whereas the aged specimen crept faster (see Fig. 9 and Table 5). This is consistent with the difference observed in the creep load line displacement between un-aged and aged conditions which was maximised for a plane stress-reference stress of 80MPa.

Fig. 10b shows the creep crack extension against the creep load line displacement for aged and un-aged P92 steels, which focuses on the early stages of testing for a critical creep load line displacement of 0.1mm of crack growth. The creep crack incubation was set to 0.1mm since this validity coincident with the change in the slope of the load line displacement curve including loading and creep (see Fig. 6a). This limit of creep crack incubation could also be set for often selected values of extension such as 0.2mm or 0.5mm [19, 34, 35, 37-42]. Fig. 10b shows that the critical creep load line displacement at incubation decreases as a result of a reduction in the level of applied stress. As shown, this limit was lower for the aged (from 0.11mm at 120MPa to 0.05mm at 60MPa) compared to un-aged specimens (from 0.17mm at 120MPa to 0.11mm at 60MPa) which is in agreement with results presented in Fig. 10a. Similar to Fig. 10a, at 80MPa plane stress-reference stress the greatest difference in the critical value of incubation between un-aged and aged conditions was observed. All the specimens followed a similar increasing rate in the propagation for cracks post 0.1mm of crack extension, except for specimen LC-3.

### 4.3.Creep Crack Incubation

Creep crack incubation times for 0.2mm and 0.1mm of crack growth as a function of plane stress-reference stress for un-aged and aged steels at 650°C are shown in Fig. 11a and Fig. 11b. Due to lack of available experimental data in the literature for creep crack incubation times for 0.1mm of growth, the comparison [2, 43] was made for only 0.2mm. It is noteworthy that creep crack incubation time reduced when larger loads were applied which for both the un-aged and aged consistent with previously represented data [2, 43]. However, as shown for the 0.2mm incubation in Fig. 11a and 0.1mm in Fig. 11b (also summarised in Table 7), thermal ageing affected the creep crack incubation by reducing this period for a given stress level compared to the un-aged steel. This difference in the incubation time between the two microstructural conditions was increased when the load was reduced for both 0.2mm (Fig. 11a) and 0.1mm (Fig. 11b) crack extension. Although the loading condition is similar for both un-aged and aged materials, the extent of the creep zones will be different. This is schematically presented where Fig. 12a and b illustrate the growth of creep zones around the crack tip arising from an increase in the applied load. The higher levels of applied load (Fig. 12a) produce a higher stress around the crack tip, so that a larger volume of the creeping zone is generated. As a consequence locally the material will creep faster which it is controlled by creep region *III*; compared to a specimen subjected to lower applied load (Fig. 12b). Fig. 12c compares the creep zones for un-aged and aged specimens comprising an identical load and crack size for both conditions. This describes material that creeps faster where aged compared to un-aged. In the creep region *II*, due to higher creep properties for the aged, faster creep deformation is observed compared to the un-aged, leading to the crack growing faster (Fig. 12c). The creep incubation properties, which are based on the relationship between the applied plane stress-reference stresses and creep crack incubation time (0.1mm), have been computed using [41]:

$$t_i = B(\sigma_{ref})^m \quad (11)$$



where  $t_i$  and  $\sigma_{ref}$  are the incubation time and reference stress (plane stress in this study), also  $B$  and  $m$  are the corresponding material constants. Eq. 11 based on data presented in Fig. 11b reveals that there is a difference between the incubation parameters of un-aged and aged steels. The constants for creep crack incubation time for 0.1mm extension are  $B = 10 \times 10^9$  ( $hrMPa^{-n}$ ) and  $m = -4.028$  for un-aged P92 steel and  $B = 4 \times 10^8$  ( $hrMPa^{-n}$ ) and  $m = -3.367$  for aged steel.

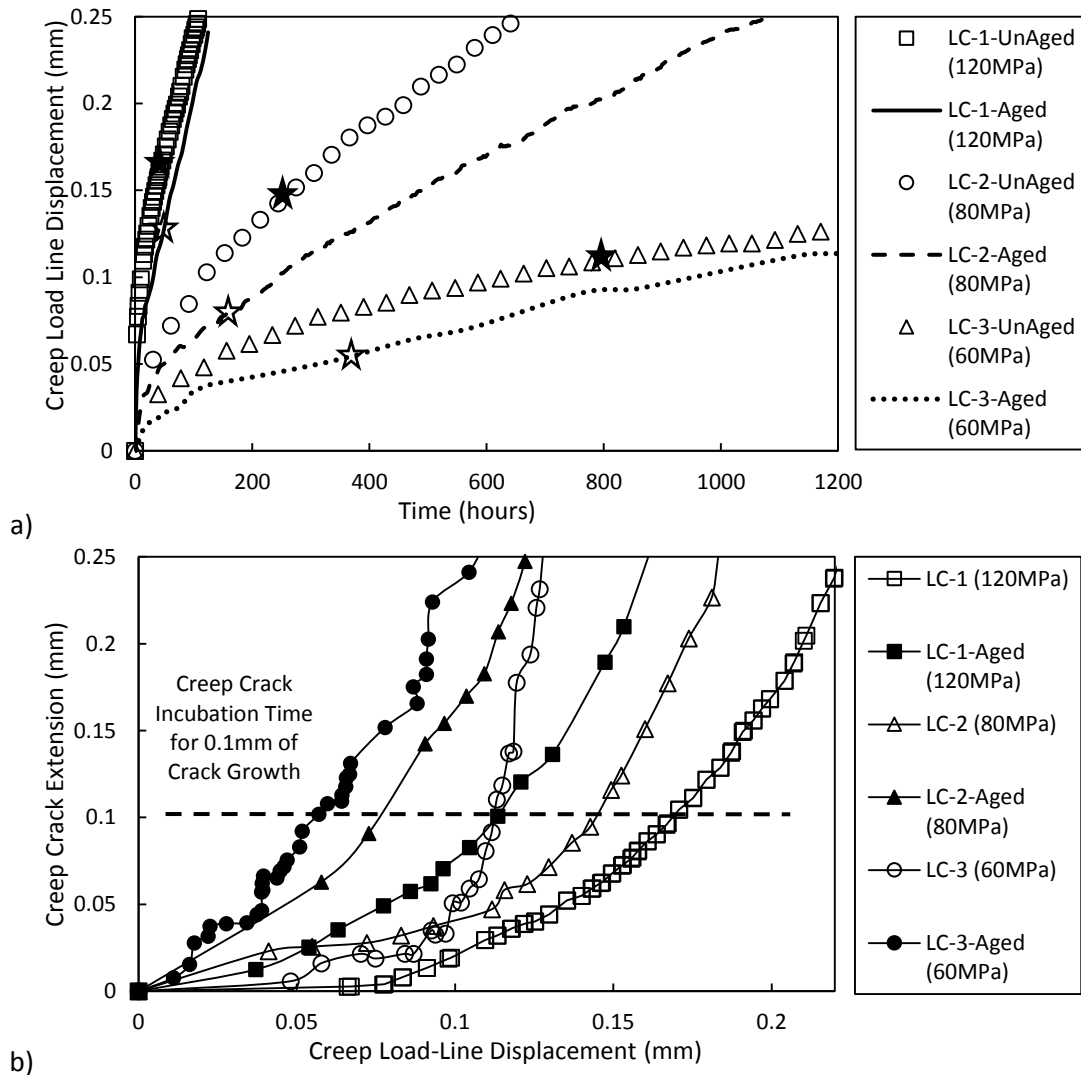


Fig. 10: a) Creep load line displacement for un-aged and aged C(T) specimen for a variety of load levels. (The hollow and solid stars represent the creep crack incubation for 0.1mm for un-aged and aged steel, respectively). b) Comparing load line displacement against creep crack length extension for aged and un-aged CT specimen under 80MPa and 120MPa reference stress. (The plane stress-reference stress indicated for each test in the brackets)

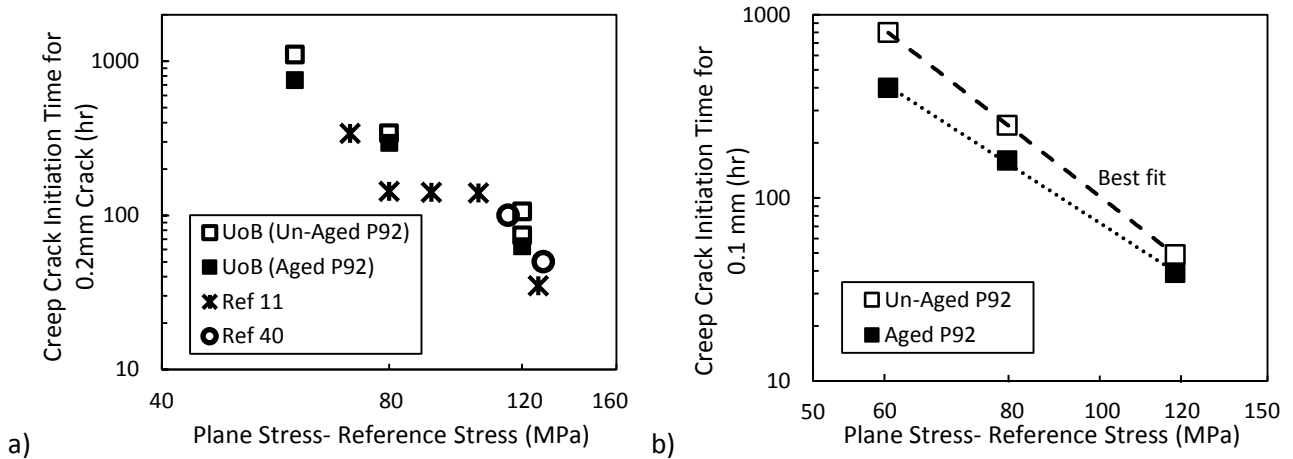


Fig. 11: Creep crack initiation time for un-aged and aged steels against the applied plane stress-reference stress; a) for 0.2mm, b) for 0.1mm

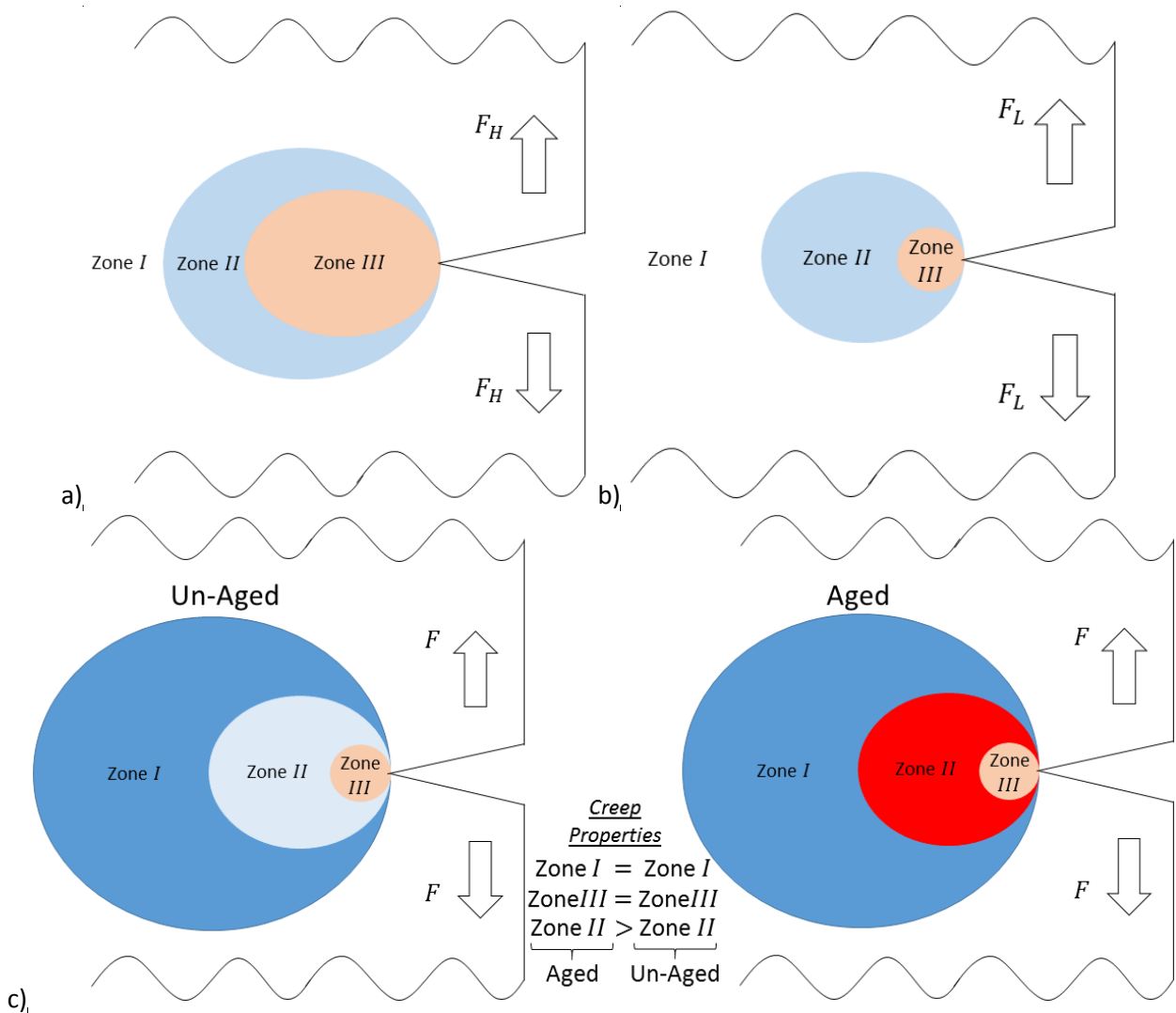


Fig. 12: Schematic illustration of creep zones (region) around a crack tip: a) low level of applied load, b) high level of applied load ( $F_L < F_H$ ), c) creep zones for un-aged and aged conditions at an identical load and crack size.

#### 4.4. Monkman-Grant Analysis

Monkman-Grant [42] provided a relationship, for metals and alloys, between minimum creep strain rate and rupture time ( $t_r$ ):

$$(\dot{\epsilon}_{min})^a \cdot t_r = C_{MG} \quad (12)$$

where  $C_{MG}$  is the Monkman-Grant constant and  $a$  is material property, normally equal to unity. It can be argued that the mechanism of creep deformation and fracture are essentially the same at that specific test condition, if the material obeys this relationship [43]. By plotting minimum creep strain rate against the rupture time for both un-aged and aged P92 steel, Monkman-Grant parameters can be derived, as shown in Fig. 13. Table 9 summarises the Monkman-Grant parameters for both un-aged and aged steels based on creep rupture data for stresses of 120MPa (located in the middle creep regime) and 170MPa (at the high creep regime), even though they are not in the same stress level.

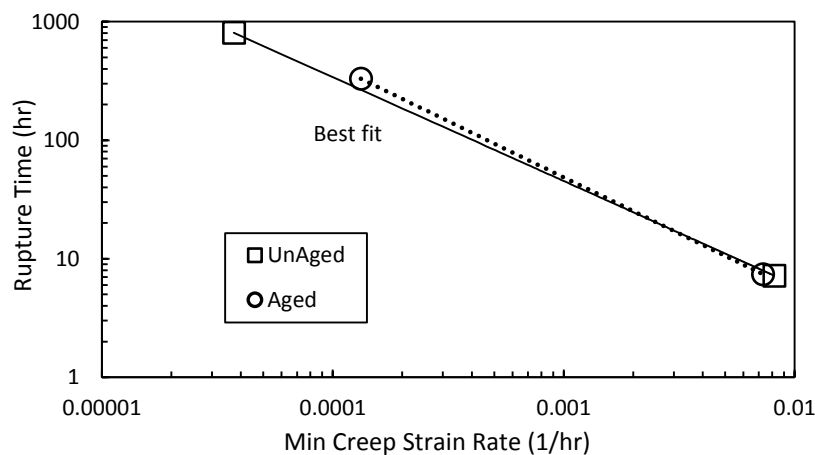


Fig. 13: The changes of minimum creep strain rate with time to rupture for un-aged and aged P92 steel at 650°C

Table 9: Monkman-Grant parameters for aged and un-aged P92 steel

	$a$	$C_{MG}$
Un-Aged P92 Steel	0.88	0.11
Aged P92 Steel	0.95	0.07

#### 4.5. Impact of Thermal Ageing

In general exposing materials to high temperature for extended periods of time modifies the microstructure and therefore the mechanical behaviour [3], [8], [4] [10]–[12], [14]. Unfortunately there is a lack of experimental data for aged P92 steel at 650°C for the extended periods of service exposure. This makes the process of comparison of experimental results and model predictions challenging. Panait et al [4] explored the effect of 10k hours of thermal ageing at 650°C for a T92 steel. Here, we compare the present data with that of Panait et al [4] to evaluate the effect of long-term ageing on creep deformation. Table 10 summarises the minimum creep strain rate for un-aged P92 steel, aged P92 (1k hours) and aged T92 steels (10k hours) [4] that has been collected over the range of stresses from 80MPa to 120MPa at 650°C. Fig. 14 shows minimum creep strain rate as a function of applied stress for un-aged and aged T92 and P92 steels at 650°C. The rate of minimum creep strain increased for the aged steel compared to un-aged for stresses exceeding 80MPa and this difference is more significant for higher applied stresses. At 120MPa, for example, minimum creep strain

rate increased by a factor of eight for aged T92 steel (10k hours of ageing) compared with un-aged while, this was almost four times higher for aged P92 steel (1k hours of ageing). It is evident that for a longer period the material is exposed to high temperature, the more the creep properties are degraded and hence the service life affected.

Table 10: Comparison of minimum creep strain rate for un-aged and aged (P92 steel for 1K hours and T92 steel [4] for 10K hours)

Stress (MPa)	80 (P92)	95 (T92)	100 (P92)	110 (T92)	120 (P92)	120 (T92)
Un-Aged	3.48E-06	6.00E-06	1.27E-05	2.10E-05	3.73E-05	2.50E-05
$\dot{\epsilon}_{min}$ (1/hr)						
1k hrs Aged	3.48E-06	----	2.64E-05	----	1.32E-04	----
10k hrs Aged	----	1.40E-05	----	9.40E-05	----	2.11E-04

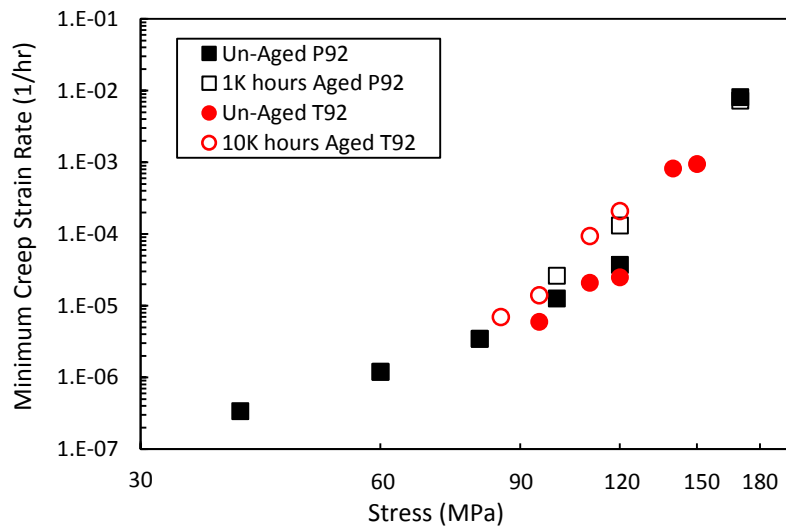


Fig. 14: Minimum creep strain rate as a function of applied stress for un-aged P92 and T92 steels ([4]), and aged P92 (1K hour) and T92 steels ([4]) (10K hour) steels at 650°C

The experimental results revealed that the thermal ageing adopted in the present work change the original creep strain curve for the P92 martensitic steel by increasing the secondary creep strain rate which is a thermal activation controlled process, but it does not affect the primary creep. Fig. 15a shows a schematic diagram to summarise effect of thermal ageing on creep deformation. Since thermal ageing affects the creep deformation over a limited range of stresses, it is vital to explore the influence on creep cracking. It is proposed that the presence of the triaxial stress field ahead of the crack tip, this has the potential to lead to the material subject to different creep stress regimes. The experimental results suggest that thermal ageing reduces the creep crack incubation time, as shown in Fig. 15b by modelling the creep crack incubation time versus stress (or load) actually an effect of ageing on creep crack incubation was observed for all the stress (or load) levels so that thermal ageing provides an almost parallel line to un-aged steel in Fig. 15b.

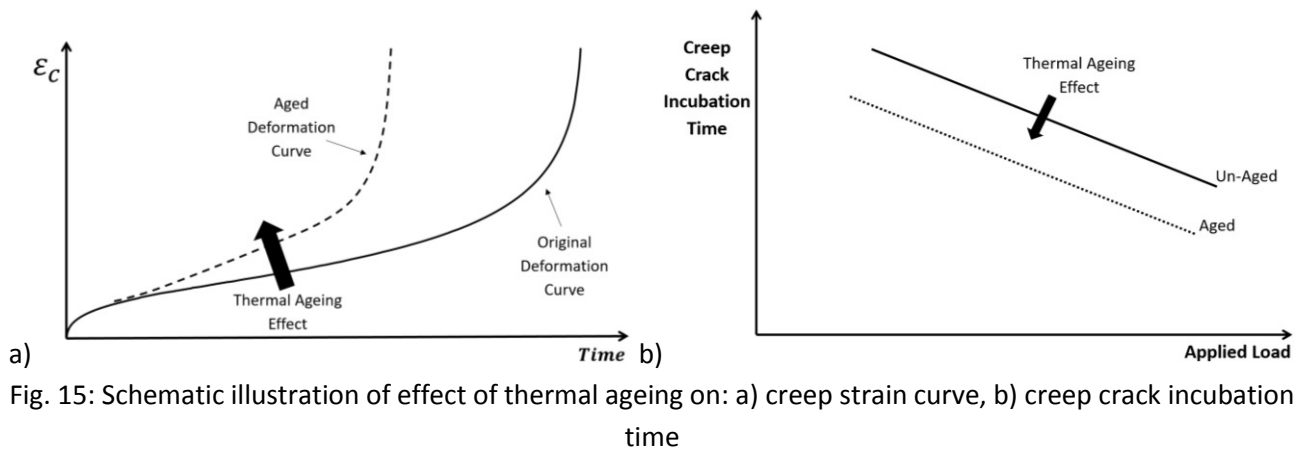


Fig. 15: Schematic illustration of effect of thermal ageing on: a) creep strain curve, b) creep crack incubation time

## 5. Conclusion

- Tensile tests conducted at temperature suggest that for the specific thermal ageing undertaken on a martensitic 9Cr1Mo (P91) steel does not affect the Young's modulus of elasticity and the yield strength, while the ultimate stress was reduced compared with the un-aged condition.
- The uniaxial creep deformation tests conducted on un-aged and aged P92 steel at 650°C revealed that there is an effect on creep behaviour over a range of stresses. The material behaviour was affected by thermal ageing over a relatively very narrow stress range between 85MPa to 140MPa, where creep life was reduced, e.g. at 120MPa, the rupture time was reduced by a factor of three.
- Thermal ageing does not affect primary creep as it does not change work hardening but modifies secondary creep and decreases the creeping life of the material. As a result, the minimum creep strain rate increased earlier failure and resulting the aged steel to creep faster compared to un-aged, and for the same stress level.
- The creep crack incubation test results showed that a crack incubated earlier for aged steel compared to un-aged steel. More distributed micro cracks were present around the crack tip in the aged test specimens compared to the un-aged.
- It was observed from uniaxial creep stress relaxation tests with elastic follow-up of 1.17 that thermal ageing does not have an effect on the creep stress relaxation.

## Acknowledgements

Saber Khayatzaeh would like to dedicate this paper to the memory of his supervisor, Professor David Smith, who was a simply wonderful colleague and friend. His sense of humour was matched by his brave, decisive and critical thinking which has had profound influence on my research. Despite our untimely goodbye, my colleagues and I will remember him forever. David Smith thanks the Royal Academy of Engineering, EDF-Energy, Rolls-Royce and the University of Bristol for supporting this work.

## References

- [1] S. Khayatzaeh, "Creep Deformation and Crack Initiation of Martensitic Steels under different Boundary Conditions," PhD Thesis, University of Bristol, 2015.
- [2] B. Dyson, "Use of CDM in materials modeling and component creep life prediction," *J. Press. Vessel Technol.*, vol. 122, no. 3, pp. 281–296, 2000.
- [3] J. Hald, "Microstructure and long-term creep properties of 9-12% Cr steels," *Int. J. Press. Vessel. Pip.*, 2008.
- [4] C. Panait *et al.*, "Long term aging effect on the creep strength of the T92 steel," in *9th Liege conference: Materials*

for *Advanced Power Engineering*, 2010.

- [5] A. Gustafson and M. Hattestrand, "Coarsening of precipitates in an advanced creep resistant 9% chromium steel-quantitative microscopy and simulations," *Mater. Sci. Eng. A*, vol. 333, no. 1–2, pp. 279–286, Aug. 2002.
- [6] H. Chilukuru *et al.*, "Coarsening of precipitates and degradation of creep resistance in tempered martensite steels," *Mater. Sci. Eng. A*, vol. 510–511, pp. 81–87, Jun. 2009.
- [7] B. F. Dyson and M. McLean, "Particle-coarsening,  $\sigma_0$  and tertiary creep," *Acta Metall.*, vol. 31, no. 1, pp. 17–27, Jan. 1983.
- [8] M. Yoshizawa, M. Igarashi, K. Moriguchi, A. Iseda, H. G. Armaki, and K. Maruyama, "Effect of precipitates on long-term creep deformation properties of P92 and P122 type advanced ferritic steels for USC power plants," *Mater. Sci. Eng. A*, vol. 510–511, pp. 162–168, Jun. 2009.
- [9] B. Chen *et al.*, "Effect of thermal ageing on creep and oxidation behaviour of Type 316H stainless steel," *Mater. High Temp.*, vol. 32, no. 6, pp. 592–606, 2015.
- [10] L. Zhao, H. Jing, Y. Han, J. Xiu, and L. Xu, "Prediction of creep crack growth behavior in ASME P92 steel welded joint," *Comput. Mater. Sci.*, vol. 61, pp. 185–193, Aug. 2012.
- [11] L. Zhao, H. Jing, L. Xu, Y. Han, and J. Xiu, "Evaluation of constraint effects on creep crack growth by experimental investigation and numerical simulation," *Eng. Fract. Mech.*, vol. 96, pp. 251–266, Dec. 2012.
- [12] T. Sakthivel *et al.*, "Creep rupture behavior of 9Cr-1.8W-0.5Mo-VNb (ASME grade 92) ferritic steel weld joint," *Mater. Sci. Eng. A*, vol. 591, pp. 111–120, Jan. 2014.
- [13] V. Sklenicka, K. Kucharova, M. Svoboda, L. Kloc, J. Bursik, and A. Kroupa, "Long-term creep behavior of 9-12%Cr power plant steels," *Mater. Charact.*, vol. 51, pp. 35–48, Aug. 2003.
- [14] M. Ohgami, H. Naoi, S. Kinbara, H. Mimura, T. Ikemoto, and T. Fujita, "Development of 9CrW Tube, Pipe and Frogging for Ultra Supercritical Power Plant Boilers," 1997.
- [15] L. Zhao, H. Jing, L. Xu, J. An, and G. Xiao, "Numerical investigation of factors affecting creep damage accumulation in ASME P92 steel welded joint," *Mater. Des.*, vol. 34, pp. 566–575, Feb. 2012.
- [16] J. S. Lee, H. G. Armaki, K. Maruyama, T. Muraki, and H. Asahi, "Causes of breakdown of creep strength in 9Cr-1.8W-0.5Mo-VNb steel," *Mater. Sci. Eng. A*, vol. 428, no. 1–2, pp. 270–275, Jul. 2006.
- [17] E. Hosseini, "prediction of long term creep rupture properties of welded joints using the results of short duration creep crack incubation tests," PhD Thesis, ETH Zurich University, 2013.
- [18] S. Khayatzadeh, D. W. J. Tanner, C. E. Truman, P. E. J. Flewitt, and D. J. Smith, "Creep deformation and stress relaxation of a martensitic P92 steel at 650°C," *Eng. Fract. Mech.*, 2017.
- [19] M. Saber, "Experimental and Finite Element Studies of Creep and Creep Crack Growth in P91 and P92 Weldments," PhD Thesis, Nottingham University, 2011.
- [20] W. Bendick, L. Cipolla, J. Gabrel, and J. Hald, "New ECCO assessment of creep rupture strength for steel grade X10CrMoVNb9-1 (Grade 91)," *Int. J. Press. Vessel. Pip.*, vol. 87, no. 6, pp. 304–309, Jun. 2010.
- [21] L. Zhao, H. Jing, L. Xu, Y. Han, and J. Xiu, "Experimental study on creep damage evolution process of Type IV cracking in 9Cr–0.5Mo–1.8W–VNb steel welded joint," *Eng. Fail. Anal.*, vol. 19, pp. 22–31, Jan. 2012.
- [22] L. Zhao, H. Jing, L. Xu, Y. Han, and J. Xiu, "Analysis of creep crack growth behavior of P92 steel welded joint by experiment and numerical simulation," *Mater. Sci. Eng. A*, vol. 558, pp. 119–128, Dec. 2012.
- [23] A. Skouras, "Generation and relaxation of residual stresses in dissimilar metal welds," PhD Thesis, University of Bristol, 2013.
- [24] P. Ennis and A. Czyrska-Filemonowicz, "Recent advances in creep-resistant steels for power plant applications," *Sadhana*, vol. 28, no. 3–4, pp. 709–730, 2003.
- [25] S. Khayatzadeh, D. W. J. Tanner, C. E. Truman, and D. J. Smith, "Effect of Elastic Follow-up on Creep Crack Incubation," *Procedia Mater. Sci.*, vol. 3, pp. 1485–1491, 2014.
- [26] E. Astm, "1457-07: standard test method for measurement of creep crack growth times in metals," *Annu. B. ASTM Stand.*, 2007.
- [27] A. Shirahatti, "A novel test rig to study the effects of elastic follow-up, long range residual stress and applied load on creep crack initiation," PhD Thesis, University of Bristol, 2014.
- [28] A. G. Miller, "Review of limit loads of structures containing defects," *Int. J. Press. Vessel. Pip.*, vol. 32, no. 1–4, pp. 197–327, Jan. 1988.
- [29] Y. Wang, "Design, Development and Experiments to Investigate the Effect of Elastic Follow-up on Creep Stress Relaxation in Austenitic Steels," PhD Thesis, University of Bristol, 2015.
- [30] Y. Q. Wang, M. W. Spindler, C. E. Truman, and D. J. Smith, "critical analysis of the prediction of stress relaxation from forward creep of type 316H austenitic stainless steel," *Mater. Des.*, vol. 95, pp. 656–668, 2016.
- [31] D. Richardot, J. Vaillant, A. Arbab, and W. Bendick, *The T92/P92 Book*. Vallourec and Mannesmann Tubes, 2000.
- [32] R. Penny and D. Marriott, *Design for creep*. Chapman & Hall, 1995.
- [33] M. Yurechko, C. Schroer, A. Skrypnik, O. Wedemeyer, and J. Konys, "Creep-to-rupture of the steel P92 at 650°C in oxygen-controlled stagnant lead in comparison to air," *J. Nucl. Mater.*, vol. 432, no. 1–3, pp. 78–86, Jan. 2013.
- [34] X. WANG, Z. SHI, Q. PAN, and H. WU, "High-temperature creep properties of fine grained heat-affected zone in P92 weldment," *Trans. Nonferrous Met. Soc. China*, vol. 19, pp. s772–s775, Dec. 2009.

- [35] E. I. Samuel, B. K. Choudhary, D. P. R. Palaparti, and M. D. Mathew, "Creep Deformation and Rupture Behaviour of P92 Steel at 923K," *Procedia Eng.*, vol. 55, pp. 64–69, Jan. 2013.
- [36] R. A. Ainsworth, "The initiation of creep crack growth," *Int. J. Solids Struct.*, vol. 18, no. 10, pp. 873–881, Jan. 1982.
- [37] A. Mehmanparast, "The influence of inelastic damage on creep, fatigue and fracture toughness," PhD Thesis, Imperial College London, 2012.
- [38] C. M. Davies, "Crack initiation and Growth at Elevated Temperatures in Engineering Steels," Imperial College London University, 2006.
- [39] A. Mehmanparast, C. M. Davies, D. W. Dean, and K. M. Nikbin, "The influence of pre-compression on the creep deformation and failure behaviour of Type 316H stainless steel," *Eng. Fract. Mech.*, vol. 110, pp. 52–67, Sep. 2013.
- [40] R. Sugiura, A. T. Yokobori, M. Tabuchi, and T. Yokobori, "Comparison of creep crack growth rate in heat affected zone of welded joint for 9%Cr ferritic heat resistant steel based on  $C^*$ ,  $d\delta/dt$ ,  $K$  and  $Q^*$  parameters," *Eng. Fract. Mech.*, vol. 74, no. 6, pp. 868–881, Apr. 2007.
- [41] Y. Wang, D. J. Smith, C. E. Truman, and A. M. Shirahatti, "Prediction of creep crack initiation under the interaction between long range residual stress and applied load," in *13th International Conference on Fracture, Beijing, China, pages 1-11, June 16-21, 2013*.
- [42] G. Sundararajan, "The Monkman-Grant Relationship," *Mater. Sci. Eng. A*, vol. 2, pp. 205–214, 1989.
- [43] D. W. J. Tanner, K. Chalk, W. Sun, P. H. Shipway, and T. H. Hyde, "A comparison of three weld consumables for P92 under creep," *Mater. High Temp.*, vol. 29, no. 4, pp. 359–367, Nov. 2012.